Biological, Medical Devices, and Systems

Rethinking Plant-Based Materials Production: Selective Growth of Tunable Materials via Cell Culture

A. L. Beckwith, J. T. Borenstein, L. F. Velásquez-García
Sponsorship: Draper Fellowship Program

Current systems for plant-based materials production are inefficient and place unsustainable demands on environmental resources. Traditionally cultivated crops present low yields of industrially useful components and require extensive post-harvest processing to remove extraneous portions of the plants. Large-scale monoculture remains the unchallenged standard for biomass production despite the negative impacts of the practice to the surrounding biome as well as a susceptibility to season, climate, and local resource availability. This work proposes a novel solution to these shortcomings based on the selective cultivation of useful, tunable plant tissues using scalable, land-free techniques. By limiting biomass cultivation to only desirable plant tissues, ex planta farming promises to improve yields while reducing plant waste and competition for arable land.

Employing a *Zinnia elegans* model system, we provide the first proof-of-concept demonstration of isolated, tissue-like plant material production by way of gel-mediated cell culture. Parameters governing cell development and morphology including hormone concentrations, medium pH, and initial cell density are optimized and implemented to demonstrate the tunability of cultured biomaterials at cellular and macroscopic scales. Targeted deposition of cell-doped, nutrient-rich gel scaffolds via injection molding and 3D bioprinting enable biomaterial growth in near-final form (Figure 1), reducing downstream processing requirements. These investigations demonstrate the implementation of plant cell culture in a new application space, propose novel methods for quantification and evaluation of cell development, and characterize morphological developments in response to critical culture parameters—illustrating the feasibility and potential of the proposed techniques.

The proposed concept of selectively grown, tunable plant materials via gel-mediated cell culture is believed to be the first of its kind. This work uniquely quantifies and modulates cell development of cultured primary plant products to optimize and direct growth of plant materials.

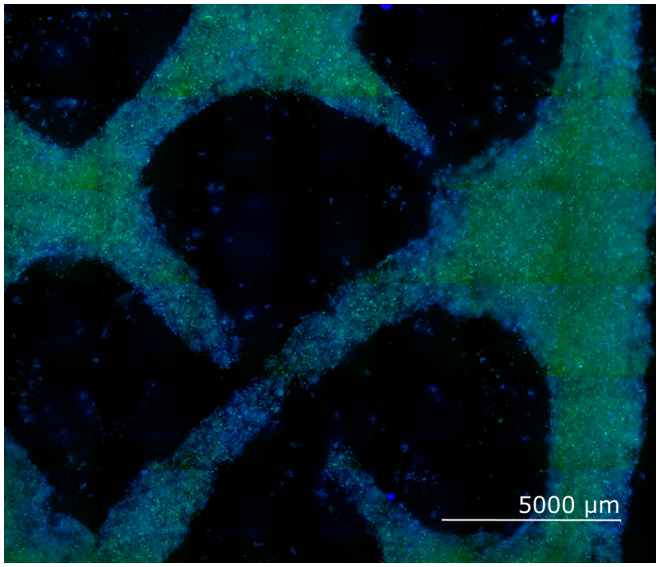

▲Figure 1: Bioprinted culture, with vascular cell types, grown to confluency.

FURTHER READING

- A. L. Beckwith, J. T. Borenstein, and L. F. Velásquez-García, "Tunable Plant-based Materials via *In Vitro* Cell Culture Using a *Zinnia Elegans* Model," *J Cleaner Production,* vol. 288, pp. 125571, Mar. 2021., DOI: 10.1016/j.jclepro.2020.125571.
- A. L. Beckwith, J. T. Borenstein, and L. F. Velásquez-García, "Monolithic, 3D-printed Microfluidic Platform for Recapitulation of Dynamic Tumor Microenvironments," *J Microelectromech* Syst, vol. 27, 6, pp.1009-1022, Oct. 2018, DOI: 10.1109/JMEMS.2018.2869327.
- A. L. Beckwith, L. F. Velásquez-García, and J. T. Borenstein, "Microfluidic Model for Evaluation of Immune Checkpoint Inhibitors in Human Tumors," *Advanced Healthcare Materials*, vol. 8, 11, pp. 1900289, Jun. 2019, DOI: 10.1002/adhm.201900289.

Absolute Blood Pressure Waveform Monitoring using Philips Ultrasound Probe

A. Chandrasekhar, A. Aguirre, C. G. Sodini, H.-S. Lee
Sponsorship: MEDRC-Philips, MIT J-Clinic, CICS

In an Intensive Care Unit (ICU), physicians use an invasive radial catheter to measure blood pressure (BP) to track the hemodynamic status of the subject, and these measurements are neither easy nor feasible to perform outside an ICU environment. In such non-ICU settings as a step-down clinical ward or an outpatient clinic, clinicians prefer to use a non-invasive arm-cuff device to measure BP. Even though these measurements are convenient, these devices cannot record the absolute BP (ABP) waveform. Hence, strong interest exists in developing a non-invasive device to monitor the ABP waveform as a quantitative option to perform rapid hemodynamic profiling of patients who cannot undergo invasive BP measurements.

This project uses a Philips ultrasound-based transducer (XL-143) to measure BP from superficial arteries (carotid and brachial) proximal to the heart. We measure the arterial diameter and blood flow velocity waveforms from these arteries; an algorithm computes BP from this data in three stages, as illustrated in Figure 1. The algorithm uses the arterial area (A) calculated from arterial diameter and the blood flow velocity (F) waveforms to estimate the height of the ABP waveform, known as pulse pressure (PP), via standard fluid dynamics principles. Further, the algorithm uses a transmission line model of the human vasculature to estimate the mean arterial pressure (MAP).

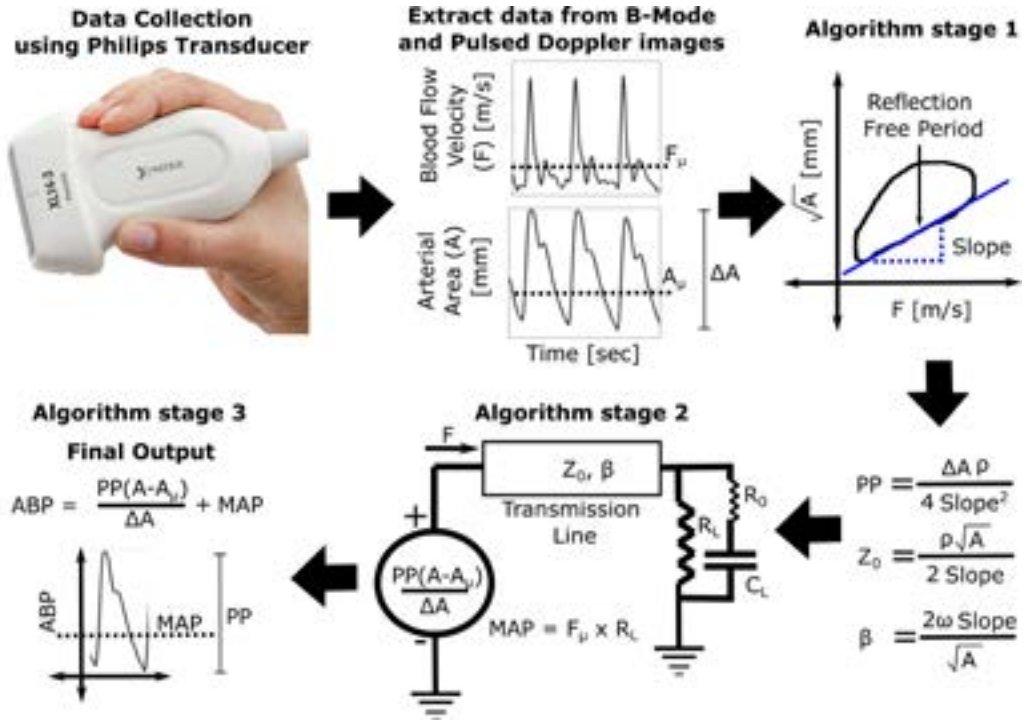

▲ Figure 1: An algorithm to estimate absolute blood pressure waveform from ultrasound signals.

FURTHER READING

- J. Seo, "A Non-invasive Central Arterial Pressure Waveform Estimation System using Ultrasonography for Real-time Monitoring," Ph.D. dissertation, Massachusetts Institute of Technology, Cambridge, 2018.

Electrochemical Neuromodulation Using Electrodes Coated with Ion-Selective Membranes

M. T. Flavin, C. Lissandrello, J. Han
Sponsorship: Draper Laboratory

Developing precise and effective means of modulating the nervous system is a major challenge in neural prostheses. While modalities such as deep brain stimulation (DBS), vagus nerve stimulation, and electric acoustic stimulation (EAS) for cochlear implants are finally being realized on the clinical level, there still remains work to be done with respect to our ultimate goal. In the Micro/Nanofluidic BioMEMS research group, we are developing a type of electrode modified with an ion-selective material that can change the concentration of chemicals around a nerve, which will enhance the level of control compared to traditional electrical stimulation.

A type of material called the ion-selective membrane (ISM) has been used in the field of analytical chemistry for decades to measure ion concentrations. These membranes are composed of a polymer matrix modified with a chemical called an ionophore, which makes them selective to a particular ion species. In work published by our group, the functionality of these electrodes was inverted, using them for electrochemical stimulation in ex vivo studies of a frog sciatic nerve (see Figure 1 from Song et al.).

As a continuation of this work, we are: (1) developing computational models that describe and predict physical behavior of chemical transport from galvanostatic operation of polymeric neutral-carrier based ion-selective membrane electrodes, (2) fabricating and characterizing practical devices for implementing ISM-based neuromodulation (see Figure 2 from Flavin et al.), and (3) employing prototype devices in *in vitro* and *in vivo* animal models. A successful implementation of this work will pave the way for more advanced operations such as central nervous system (CNS) intervention.

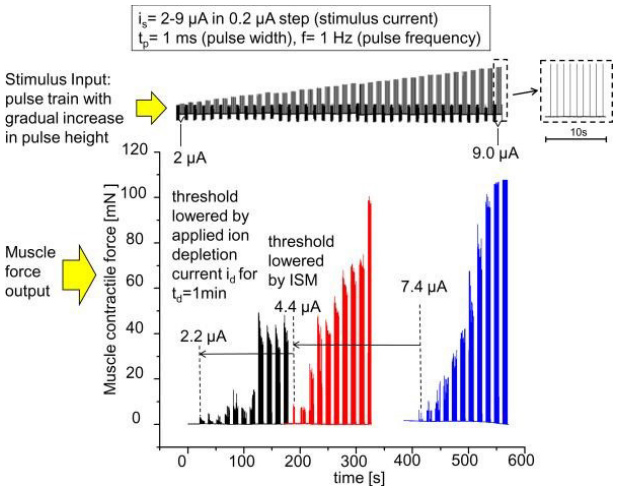

▲Figure 1: Comparison of excitability of the frog sciatic nerve without and with modulating Ca2+ ion concentration. This represents one of the current applications of the ion-selective membrane (see Song et al.).

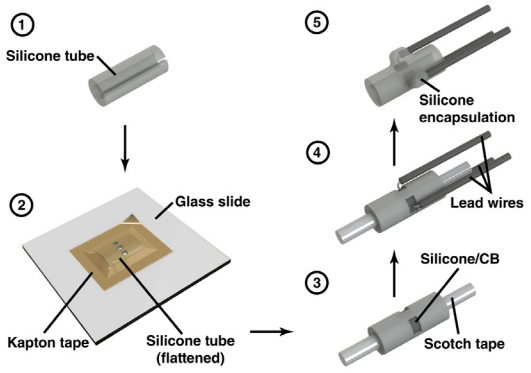

▲Figure 2: Step-by-step fabrication of rapid manufactured cuff electrodes (Flavin et al.). We developed this technology to support our in vivo work.

FURTHER READING

- Y. A. Song, R. Melik, A. N. Rabie, et al. "Electrochemical activation and inhibition of neuromuscular systems through modulation of ion concentrations with ion-selective membranes," *Nature Materials*, vol. 10, pp. 980-986, Oct. 2011.
- M. T. Flavin, M. A. Paul, A. S. Lim, et al. "Rapid and low cost manufacturing of cuff electrodes," *Frontiers in Neuroscience*, vol. 15, p.

Ultrasound-Based Cerebral Arterial Blood Flow Measurement

S. M. Imaduddin, T. Heldt
Sponsorship: Analog Devices, Inc.

Ultrasound-based cerebral blood flow (CBF) monitoring is vital in the diagnosis and treatment of a variety of acute neurologic conditions. While flow velocity can be measured using Doppler ultrasound, accurate CBF measurement is difficult as vessel diameters cannot be determined reliably due to acoustic aberrations introduced by the skull and because cranial attenuation necessitates low frequency (1-2 MHz) insonation with poor spatial resolution.

We have developed a CBF estimation technique that achieves the spatial resolution required for CBF determination by estimating the point spread function of the imaging system. The received data are then deconvolved to increase spatial resolution, and a correction is applied to account for cranial aberrations. Doppler data were collected from phantom blood vessels with diameters between 2 and 6 mm over a 150-mL/min range using a clinical ultrasound device. Our method achieved an RMSE of 26 mL/min, within acceptable range for cerebral perfusion monitoring at the bedside.

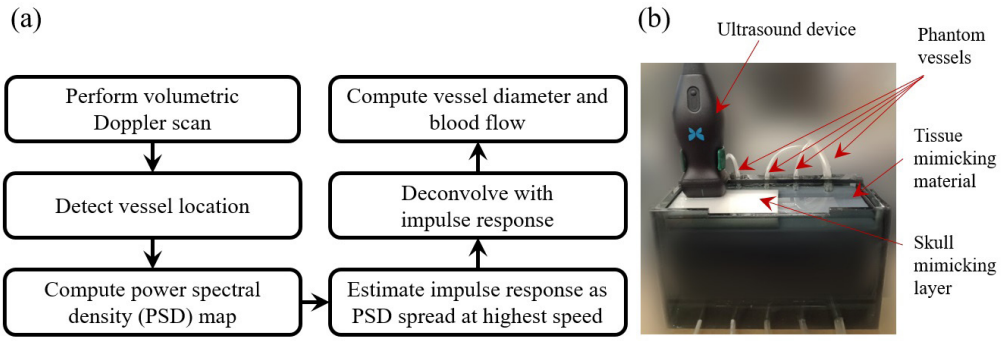

▲ Figure 1: (a) Flow chart of proposed measurement technique, and (b) Flow phantom used to test our method.

Force-Coupled Ultrasound for Noninvasive Venous Pressure Assessment

A. Jaffe, B. Anthony
Sponsorship: MEDRC-Philips

Congestive heart failure is a clinical syndrome that affects about 6 million people and accounts for about 1 in 9 deaths in the United States. In this condition, the pumping ability of the heart decreases, causing a buildup of blood volume and pressure in the venous system as it returns blood to the heart. This buildup further decreases the pumping ability of the heart by over-stretching its ventricles. Additionally, increased venous pressure can lead to fluid migrating from the veins to the interstitial space, which is called edema. Left unchecked, edema can lead to death. Proper administration of diuretic drugs can allow venous pressure to drop back down by lowering intravascular volume, which will improve a patient's condition. However, thus far, only invasive catheterization can produce an accurate and reliable venous pressure measurement.

Our goal is to produce an accurate, noninvasive means of assessing venous pressure by means of force-coupled ultrasound. By positioning our force-coupled ultrasound probe at the base of the neck, we can observe the compression of the internal jugular vein, which returns blood from the cerebral vasculature to the heart. Unlike in the case of an artery, we can safely observe compression from zero force all the way to complete occlusion of the vein. We can also observe compression of the internal jugular vein while increasing its pressure with the Valsalva maneuver, exhalation against a closed airway, and while decreasing its pressure by elevating it above the supine position. We expect these observations to give us excellent insight for our computational models to accurately assess venous pressure.

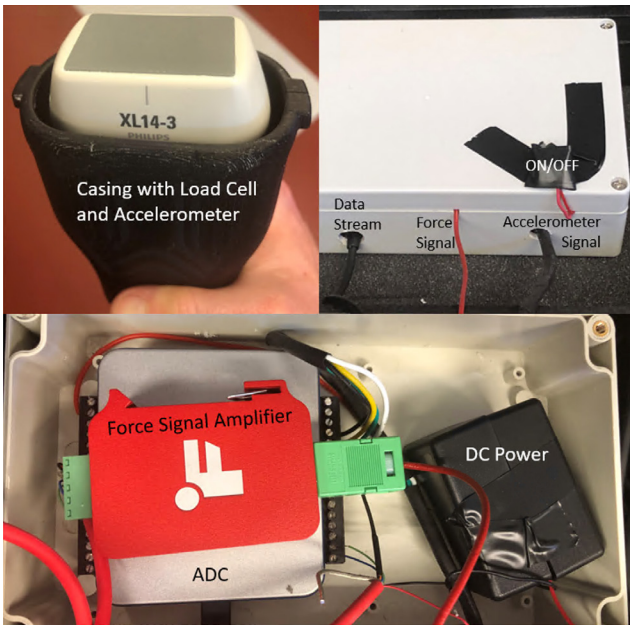

▲Figure 1: Top left: Custom-made force-coupled ultrasound casing for Philips XL14-3 xMATRIX ultrasound probe. Top right: Closed electronics box with force and accelerometer analog inputs from the casing and data streaming to a tablet for data collection and display. Bottom: Electronics box components consisting of the DC power source of two series 9V batteries, the force signal amplifier, and the multi-channel analog-to-digital converter.

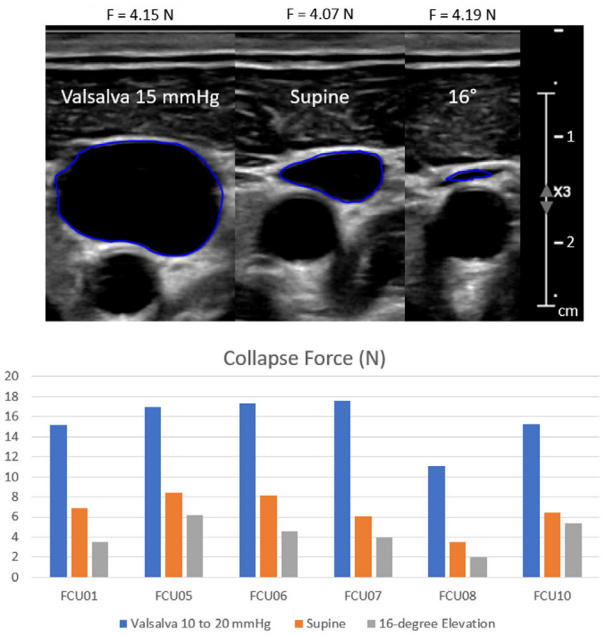

▲Figure 2: Top: Merged force-coupled ultrasound images of the segmented internal jugular vein in the same individual during a Valsalva maneuver with an airway pressure of 15 mmHg (left), during normal breathing while lying flat (middle), and during normal breathing while elevated at an angle of 16 degrees above horizontal or supine position (right). Bar graph showing the force necessary to occlude different individuals' internal jugular veins at different venous pressures.

An Electrokinetic-Based Concentrator for Ultra-Low Abundant Target Detection

H. J. Kwon, E. Wynne, J. Han
Sponsorship: Federal Drug Administration, SMART CAMP

The recent COVID-19 outbreak has sparked urgent interest in rapid and reliable viral identification. In fact, this is a recurring challenge in many other pathogen detection and diagnostics, where only a few target viruses or bacterial cells are present in milliliters or even liters of volume, necessitating that a large volume of the sample must be concentrated for the targets to be introduced into the downstream detection system. Unfortunately, due to the size of the virus or biomolecule, concentrating or retrieving the virus or biomolecule with a filter, ultracentrifuge, or any kind of method is extremely hard.

Figure 1 (a) shows the purpose of this work and the overall concept. This technology is based on microfluidic devices that couple microchannel and cation exchange membrane (CEM) to play an electrophoretic force off a hydraulic drag force to enable charge-based concentration, without any physical filter. Under the electric field, the virus experiences the electrophoretic force and hydraulic drag force at the same time. The electrophoretic force is driven by the intensive electric field focused near the CEM while drag force is driven simply by the hydraulic flow.

Efforts are being made to build electrokinetic concentrators using materials and processes that are more robust and scalable than those of traditional microfluidics. Instead of using polydimethylsiloxane (PDMS) that is patterned using photolithography, one can laser etch channels and ports into acrylic polymethyl methacrylate (PMMA). Thin adhesive films can have custom patterns cut into them using a digital die cutter and then be used to bond PMMA layers and seal channels. Designing the device in manner seen in Figure 1b also allows the use of ion- exchange membranes that are commonly used in electrodialysis and fuel cell systems, meaning these materials are robust and relatively inexpensive.

FURTHER READING

- H. J. Kwon, B. Lenneman, T. K. Lu, K. Choi, and J. Han, "An Electrokinetic-Based Large Volume Concentrator for Ultra-Low Abundant Target Detection," *uTAS*, pp. 35–36, 2020.

Micro/Nanofluidic Technologies for Next-Generation Biomanufacturing

T. Kwon, K. Choi, Z. Sun, J. Han
Sponsorship: The National Institute for Innovation in Manufacturing Biopharmaceuticals, U.S. Food and Drug Administration

Biomanufacturing of therapeutic proteins and vaccines is crucial for modern medicine. Recently, the biopharmaceutical industry started to focus more on process intensification through continuous biomanufacturing. New therapeutic modalities such as cell and gene therapies are rapidly emerging as well. Accordingly, it has become increasingly important for biomanufacturers to improve manufacturing efficiency, quality, and safety. Compared to conventional biomanufacturing technologies, micro/nanofluidic technologies can contribute to the improvement with their unique advantages. Here, we introduce our new micro/nanofluidic technologies for efficient, high-quality, and safe biomanufacturing.

First, we developed spiral microfluidic devices for reliable and efficient perfusion culture and adventitious agent (AA) clearance. The devices enable size-based cell sorting without any physical barriers, so that mammalian cells can be continuously separated from cell culture. Using this feature, the spiral device was used for 1) cell retention for perfusion culture and 2) rapid AA clearance (Figure 1). This microfluidic technology could overcome the limitations (biofouling, cell damage) of conventional cell separation techniques (e.g., membrane-based filtration, centrifugation).

Second, we introduce a new nanofluidic device for monitoring critical quality attributes (purity, binding affinity, glycosylation, etc.) of antibody therapeutics during biomanufacturing. The device has a nanofilter array and enables continuous-flow size or charge-based protein separation. Using this device, we demonstrated a fully automated continuous online protein-size monitoring during continuous perfusion culture. We are currently expanding the capability of the nanofluidic device to monitor binding affinity and glycosylation of antibodies at real-time speed (Figure 2). The technology could complement conventional protein-quality-monitoring equipment while producing a large amount of information about biologics quality.

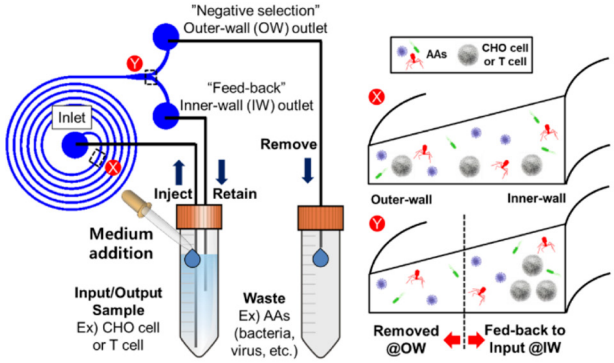

▲ Figure 1: AA clearance using a spiral microfluidic device. AAs are removed towards the waste stream constantly while CHO cells or T-cells are retained and fed back to the input. are retained and fed back to the input.

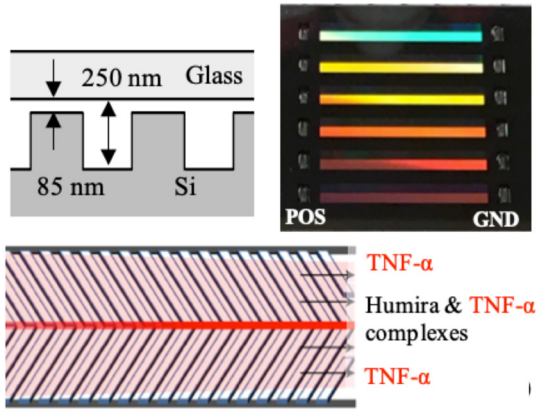

▲ Figure 2: Continuous monitoring of protein quality using a nanofluidic device. The device has a nanofilter array (85-nm shallow and 250-nm deep regions). It can concentrate Humira and TNF-alpha bound complexes.

FURTHER READING

- T. Kwon, H. Prentice, J. D. Oliveira, N. Madziva, M. E. Warkiani, J.-F. P. Hamel, and J. Han, "Microfluidic Cell Retention Device for Perfusion of Mammalian Suspension Culture," *Scientific Reports*, vol. 7, 6703, Jul. 2017.
- K. Choi, H. Ryu, K. J. Siddle, A. Piantadosi, L. Freimark, D. J. Park, P. Sabeti, and J. Han, "Negative Selection by Spiral Inertial Microfluidics Improves Viral Recovery and Sequencing from Blood," *Analytical Chemistry*, vol. 90, no. 7, pp. 4657–4662, Mar. 2018.
- T. Kwon, S. H. Ko, J.-F. P. Hamel, and J. Han, "Continuous Online Protein Quality Monitoring during Perfusion Culture Production Using an Integrated Micro/Nanofluidic System," *Analytical Chemistry*, vol. 92, no. 7, pp. 5267–5275, Mar. 2020.

Measuring Eye Movement Features using Mobile Devices to Track Neurodegenerative Diseases

H.-Y. Lai, C. G. Sodini, T. Heldt, V. Sze
Sponsorship: MIT-IBM Watson AI Lab

Current clinical assessment of neurodegenerative diseases (e.g., Alzheimer's disease) requires trained specialists, is mostly qualitative, and is commonly done only intermittently. Therefore, these assessments are affected by an individual physician's clinical acumen and by a host of confounding factors, such a patient's level of attention. Quantitative, objective, and more frequent measurements are needed to mitigate the influence of these factors.

A promising candidate for a quantitative and accessible diseases progression monitor is eye movement. In the clinical literature, an eye movement is often measured through a pro/anti-saccade task, where a subject is asked to look towards/away from a visual stimulus. Two features are observed to differ significantly between healthy subjects and patients: reaction time (time difference between a stimulus presentation and the initiation of the corresponding eye movement) and error rate (the proportion of eye movements towards the wrong direction). However, these features are commonly measured with high-speed, IR-illuminated cameras, which limits accessibility. A portable measurement system is required to track them longitudinally.

Previously, we enabled ubiquitous tracking of eye-movement features by enabling app-based measurements of visual reaction time and error rates. In this work, we further show how we learn potential trends in these eye-movement features using Gaussian process modeling. Such modeling has allowed us to discover subjects' task-performing strategies such as trading off between speed and accuracy. We hope that once we have collected data from patients, we can use the model to a) compare the trends of the features with the clinical assessments, b) distinguish the effect of strategies from the effect of disease progression, and c) evaluate the potential to use our system to track disease progression more frequently and widely than previously possible.

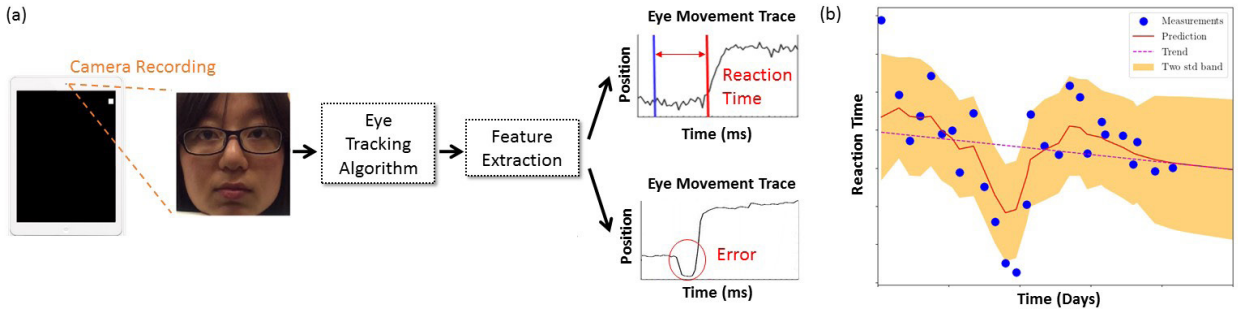

▲ Figure 1: (a) Our measurement system includes the tablet-based video recording, an eye tracking algorithm, and feature extraction algorithms. (b) Example reaction-time measurements from a subject and the trend learned from the data.

FURTHER READING

- H.-Y. Lai, G. Saavedra-Peña, C. G. Sodini T. Heldt, and V. Sze, "App-based Saccade Latency and Error Determination Across the Adult Age Spectrum," *arXiv:2012.09723 [q-bio.NC]*, 2020.
- H.-Y. Lai, G. Saavedra-Peña, C. G. Sodini, V. Sze, and T. Heldt, "Measuring Saccade Latency Using Smartphone Cameras," *IEEE Journal of Biomedical and Health Informatics*, vol. 24, no. 3, pp. 885-897, 2020.
- H.-Y. Lai, G. Saavedra-Peña, C. G. Sodini, T. Heldt, and V. Sze, "Enabling Saccade Latency Measurements with Consumer-grade Cameras," *Proc. IEEE International Conference on Image Processing (ICIP)*, pp. 3169-3173, 2018.

A Comparison of Microfluidic Methods for High-Throughput Cell Deformability Measurements

M. Urbanska, H. Muñoz, J. Bagnall, O. Otto, S. R. Manalis, D. Di Carlo, J. Guck
Sponsorship: NIH, German Federal Ministry of Research and Education

The mechanical phenotype of a cell is an inherent biophysical marker of its state and function, with many applications in basic and applied biological research. Microfluidics-based methods have enabled single-cell mechanophenotyping at throughputs comparable to those of flow cytometry. As shown in Figure 1, we present a standardized cross-laboratory study comparing three microfluidics-based approaches for measuring cell mechanical phenotype: constriction-based deformability cytometry (cDC), shear flow deformability cytometry (sDC), and extensional flow deformability cytometry (xDC). All three methods detect cell deformability changes induced by exposure to altered osmolarity. However, a dose-dependent deformability increase upon latrunculin B-induced actin disassembly was detected only with cDC and sDC, which suggests that when cells are exposed to the higher strain rate imposed by xDC, cellular components other than the actin cytoskeleton dominate the response. The direct comparison presented here furthers our understanding of the applicability of the different deformability cytometry methods and provides context for the interpretation of deformability measurements performed using different platforms.

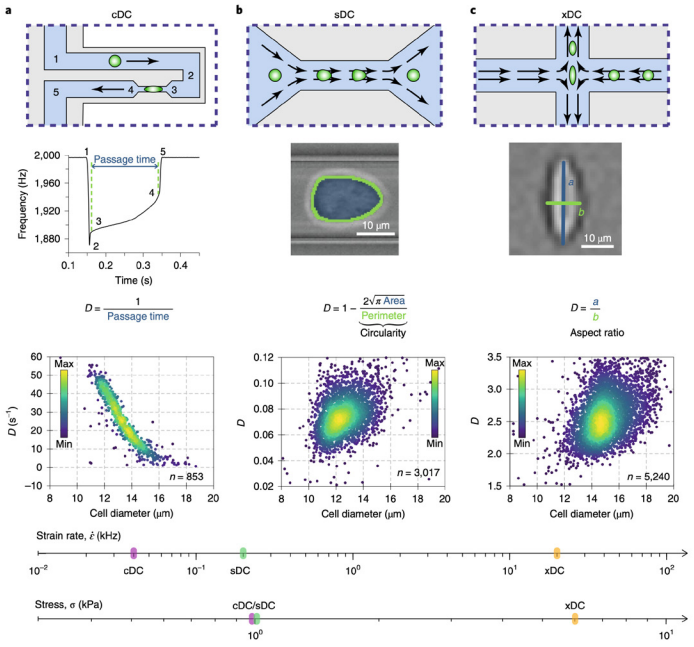

▲ Figure 1: Comparison of the microfluidics-based approaches for the determination of cell deformability used in this study. a–c, Operation principle of cDC (a), sDC (b), and xDC (c). Schematic representation of the chip geometries used in the respective methods (top row). Overview of how the deformability, D, is defined for each method (middle row). The numbers 1–5 in the plot of frequency versus time correspond to the cell positions in the cDC microchannel indicated in the scheme above. Representative scatter plots of D versus cell diameter from the measurements of untreated HL60 cells (bottom row); n indicates number of cells; the measurements were repeated a total of 10, 9, and 8 times for cDC, sDC, and xDC, respectively. The color map corresponds to event density. The strain rate and stress applied to the cells in cDC, sDC, and xDC are indicated on the corresponding axes at the bottom of the panel.

FURTHER READING

- M. Urbanska, H. Muñoz, J. Bagnall, O. Otto, S. R. Manalis, D. Di Carlo and J. Guck, "A Comparison of Microfluidic Methods for High-throughput Cell Deformability Measurements," *Nature Methods*, vol. 17, no. 6, pp. 587–593, Jun. 2020.

Electronics for Transparent, Long-Lasting Respirators

S. Orguc, A. Wentworth, J. Byrne, J. Sands, S. Maji, C. Tov, S. Babaee, H. Huang, H. Boyce, P. R. Chai, S. Min, C. Li, J. N. Chu, A. Som, S. L. Becker, M. Gala, A. P. Chandrakasan, G. Traverso
Sponsorship: NIH

The use of personal protective equipment (PPE), including the N95 respirators and surgical masks, is essential in reducing airborne disease transmission, particularly during the COVID-19 pandemic. Unfortunately, there has been a shortage of PPE since the beginning of the pandemic. Also, the available N95 masks have major limitations, including masking facial features, waste, and lack of integrity after decontamination, forcing researchers to find alternatives.

This work presents a transparent, elastomeric, adaptable, long-lasting respirator with an integrated biometric interface. The mask is made mostly of silicon rubber and comes with two replaceable filter cartridges. The electronic interface uses one of the filter insert locations to measure temperature, humidity, pressure, and air quality. The system uses Bluetooth Low Energy and sends real-time sensor data to a phone or a computer. The data can be used to inform the user regarding mask fit, fatigue, mask condition, and potential diagnostic information.

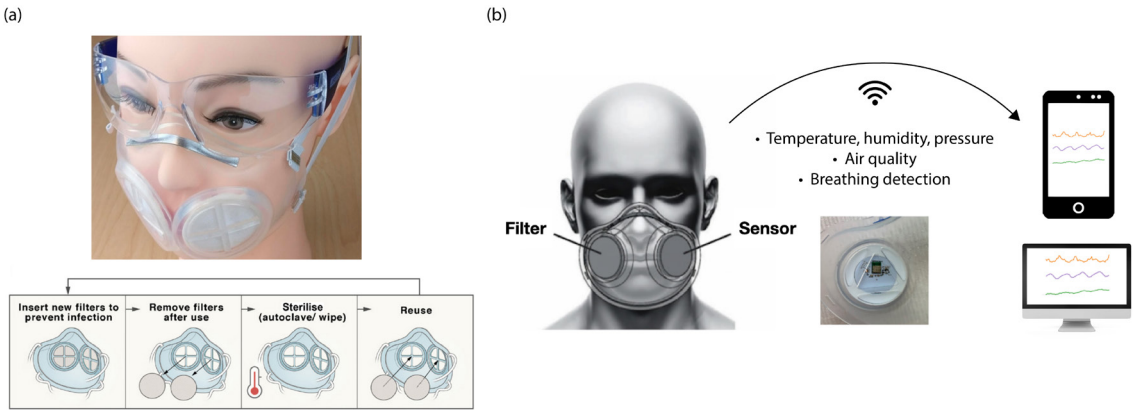

▲ Figure 1: (a) The respirator prototype. (b) System overview for the biometric sensor interface and the wireless operation.

Self-Editing or "Lamarckian" Genomes Using the Bio/Nano TERCOM Approach

J. Protz
Sponsorship: Protz Lab Group; BioMolecular Nanodevices, LLC

Gene editing has been an area of active investigation for many decades. Some approaches introduce permanent edits; others modify expression. In this work, conceptually, cells or cell-free reactions estimate their location by correlating the evolution of their sensed fluid environment (e.g., temp., salinity, sugar, pH, ion concentration, etc.) against an embodied map and then self-edit the content of their genomes in a way that depends on said estimate; editing the genome shifts the expressed phenotype and the heritable genotype. This approach is related to terrain contour matching (TERCOM), a technique used in air navigation. Current efforts focus on a reaction mixture containing a plasmid that experiences path-dependent self-edits while en route to a target site. As envisioned (see Figure 1), a read-only so-called "junk DNA" segment of a plasmid transcribes into mRNA strands having coding heads and consumable tails; the tails are attacked by an exonuclease, the activity of which depends jointly on removed monomer species and local ion concentration (or another environmental variable), causing the tails to function as path-sensitive fuses and the mix of surviving mRNA to depend on the path. The surviving mRNA is reverse-transcribed into DNA and integrated as expressible genes in a read-write portion of the plasmid; concurrent random erasures keep overall length roughly constant. In this process, the genetic composition of the read-write region evolves with the changing environmental path. A related heritage effort explores drug delivery using particles that exhibit path-dependent doses or conformation. The current and heritage efforts build on prior study by the PI and his group of nanoparticles that record the trajectory of their environment. An experimental apparatus has been designed to test these various TERCOM-like reaction mixtures. Progress on the present effort may allow the engineering of organisms that exhibit Lamarckian evolution or gene therapies that confer this ability.

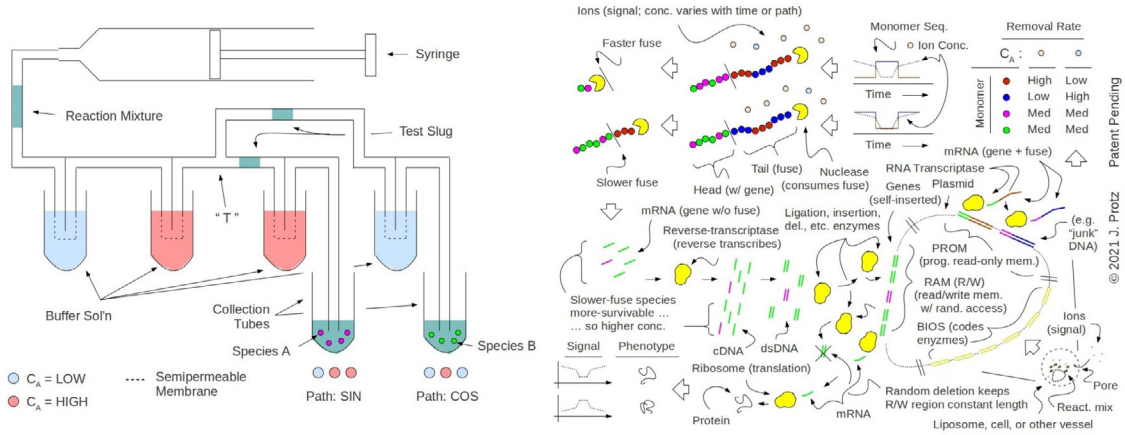

▲ Figure 1: Illustration of concept: (a) apparatus to test sensitivity to path of reaction and delivered genome; (b) nuclease with environmental and substrate sensitivity consumes transcribed RNA's protective tail; RNA with path-matching tails survives and is reverse- transcribed and incorporated into plasmid DNA, causing genetic composition of plasmid to depend on path.

FURTHER READING

- J. Protz, "Methods and Compositions for Targeted Delivery, Release, and/or Activity," *Int'l. Patent App.* PCT/US2021/016111, 1 Feb 2021. See also Int'l Patent App. PCT/US2019/031395 (WO/2019/217601), May 8, 2019.
- J. Protz, M. Tanner, E. Vasievich, A. Lee, A. Jain, and T. LaBean, "Bio-Nanoparticle for Drug Delivery Using TERCOM," *Proc. MIT MTL Annual Research Conf. (MARC 2021)*, S6.06, p. 32, 2021.
- M. Tanner, E. Vasievich, and J. Protz, "Experimental Demonstration of Lossy Recording of Information into DNA," *Proc. SPIE 7679, Micro- and Nanotechnology Sensors, Systems, and Applications II*, 767920, doi: 10.1117/12.858775; https://doi.org/10.1117/12.858775, 2010.

Balancing Actuation Energy and Computing Energy in Motion Planning

S. Sudhakar, V. Sze, S. Karaman
Sponsorship: NSF, Cyber-Physical Systems (CPS) Program, grant no. 1837212

Inspired by emerging low-power robotic vehicles such as insect-size flyers, high-endurance autonomous blimps, and chip-size satellites, we identify a new class of motion-planning problems in which the energy consumed by the computer while planning a path can be as large as the energy consumed by the actuators during the execution of the path. Figure 1 shows how the energy to move one meter on various low-powered robotic platforms is of a similar magnitude to the energy to compute one second on various embedded computers. As a result, minimizing energy requires minimizing both actuation energy and computing energy since computing energy is no longer negligible. Figure 2 shows average actuation energy and computing energy curves for a selected robotic platform and a computing platform. Here, minimizing only actuation energy, as is conventionally done, does not minimize total energy. Instead, stopping computing earlier and accepting a higher actuation energy cost for a lower computing energy cost minimizes total energy.

We propose the first algorithm to address this new class of motion planning problems, called Computing Energy Included Motion Planning (CEIMP). CEIMP operates similarly to other anytime planning algorithms, except that it stops when it estimates that while further computing may save actuation energy by finding a shorter path, the additional computing energy spent to find that path will negate those savings. We evaluate CEIMP on realistic computational experiments involving 10 MIT building floor plans, and CEIMP outperforms the average baseline of using maximum computing resources. In one representative experiment on an embedded CPU (ARM Cortex A-15), for a simulated vehicle that uses one Watt to travel one meter per second, CEIMP saves 2.1-8.9x of the total energy on average across the 10 floor plans over the baseline, which translates to missions that can last equivalently longer on the same battery.

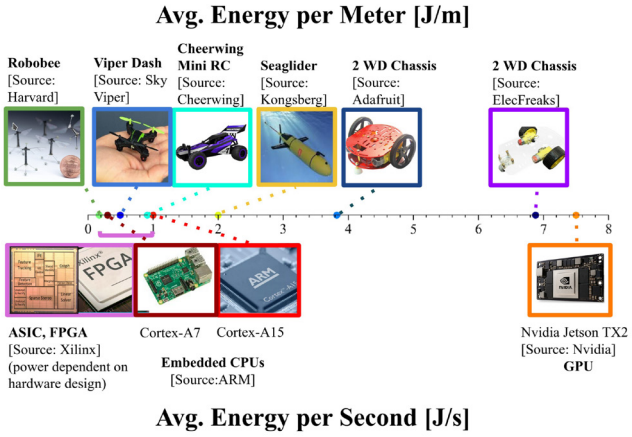

▲Figure 1: The energy-per-meter various low-power robotic platforms consume to actuate is on a similar magnitude as the energy-per-second that embedded computers consume to compute.

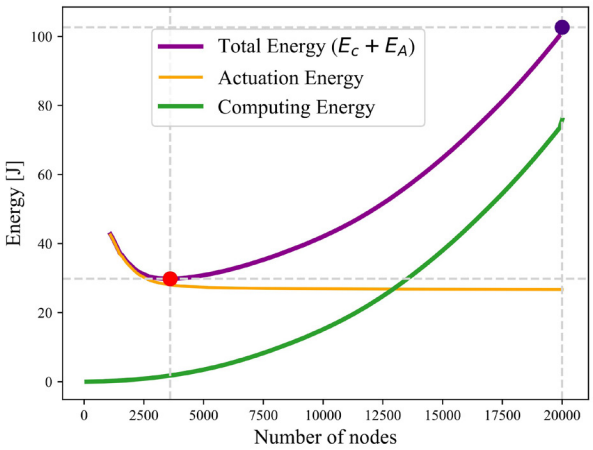

▲Figure 2: Average computing energy, actuation energy, and total energy (computing + actuation) curves vs. nodes in a sampling-based motion planner.

FURTHER READING

- S. Sudhakar, S., Karaman, S., and V. Sze, V. "Balancing Actuation and Computing Energy in Motion Planning," *2020 IEEE International Conference on Robotics and Automation (ICRA)* pp. 4259-4265, May 2020.

Absolute Blood Pressure Measurement using Machine Learning Algorithms on Ultrasound-based Signals

H. Wang, A. Chandrasekhar, A. Aguirre, C. G. Sodini, H.-S. Lee, S. Han
Sponsorship: MIT J-Clinic, MEDRC-Analog Devices, NSF CAREER Award, DARPA Software-Defined Hardware

Hypertension, or high blood pressure (BP), is a major cardiovascular risk factor. Therefore, measuring BP is of significant clinical value. At present, there are a few disadvantages for devices that measure a patient's BP. For instance, in an Intensive Care Unit (ICU), physicians use an invasive radial catheter to measure BP, which is not feasible outside an ICU. In non-ICU settings, clinicians use a non-invasive arm-cuff device to measure BP. This is convenient but can provide only a systolic and a diastolic pressure value and does not output the absolute BP (ABP) waveform. These devices also neglect the dynamic nature of the arterial system as they do not measure the morphology of the BP waveform, which may contain information on the underlying pathophysiology.

In this work, we propose a *non-invasive* way to get BP waveform with blood flow velocity and arterial area obtained from non-invasive ultrasound signals. One key drawback of the ultrasound-based device is that the output BP waveform has an arbitrary reference, so we have to estimate the mean arterial pressure (MAP). We propose to use a machine learning model containing 1D convolution and Transformer encoder layers to regress the MAP accurately. The input features are arterial area, flow velocity, and several other scalar features such as pulse wave velocity and pulse pressure. They are first embedded into a 512-dimension vector. Then, the convolution layers perform feature extractions, and a transformer models the relationship between time steps. We perform the training on the Pulse Wave Database (PWDB) synthetic dataset and test on seven real patients. The model provides accurate results, with mean absolute error 2.6 mmHg and std 2.1 mmHg. This algorithm has large potential to make affordable BP waveform measurements accessible to everyone.

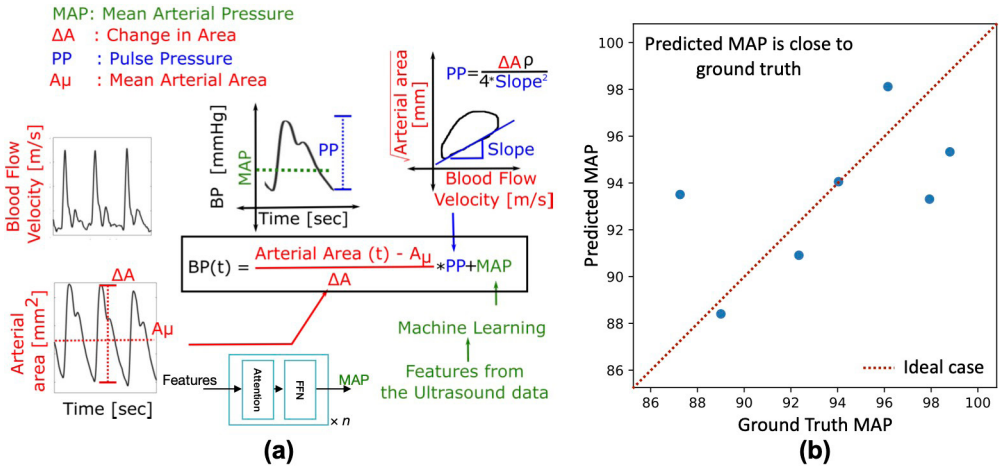

▲ Figure 1: (a) The whole pipeline of using a machine learning based algorithm to get BP waveforms from ultrasound data, and (b) predictions of the machine learning model are very accurate, with mean absolute error 2.6 mmHg and std 2.1 mmHg.

FURTHER READING

- P. H. Charlton, J. Mariscal Harana, S. Vennin, Y. Li, P. Chowienczyk, and J. Alastruey, "Modeling Arterial Pulse Waves in Healthy Aging: A Database for in Silico Evaluation of Hemodynamics and Pulse Wave Indexes," *Am J Physiol Heart Circ Physiol.*, vol. 317, no. 5, pp. H1062-H1085, 2019.
- H. Wang, Z. Wu, Z. Liu, H. Cai, L. Zhu, C. Gan, and S. Han, "Hat: Hardware-aware Transformers for Efficient Natural Language Processing," *ACL*, pp. 7675–7688, Jul. 2020.

Analytical and Numerical Modeling of an Intracochlear Hydrophone for Fully Implantable Assistive Hearing Devices

J. Z. Zhang, B. G. Cary, E. S. Olson, H. H. Nakajima, J. H. Lang
Sponsorship: NIH/NIDCD, NSF GRFP

Cochlear implants with fully implantable microphones would allow directional and focused hearing by taking advantage of ear mechanics. They would be usable in almost all environmental conditions throughout the day and night. Current implantable microphones suffer from unstable mechanics, poor signal-to-noise ratio (SNR), and low bandwidth.

In this work, we used analytical modeling, a finite element model, and experiments to design a polyvinylidene (PVDF) intracochlear hydrophone for high-bandwidth sensitivity, surgical viability, and improved SNR by electrical shielding and circuit design. Our analysis shows that the copolymer PVDF-TrFE should be used due to its higher hydrostatic sensitivity, the area of the sensor should be maximized to maximize gain, and the length should not exceed a maximal value determined by the bandwidth requirement. A short-circuit topology charge amplifier maximizes the SNR of the sensor by minimizing noise and attenuating electromagnetic interference by shielding. These advances in sensor performance bring fully implantable systems closer to reality.

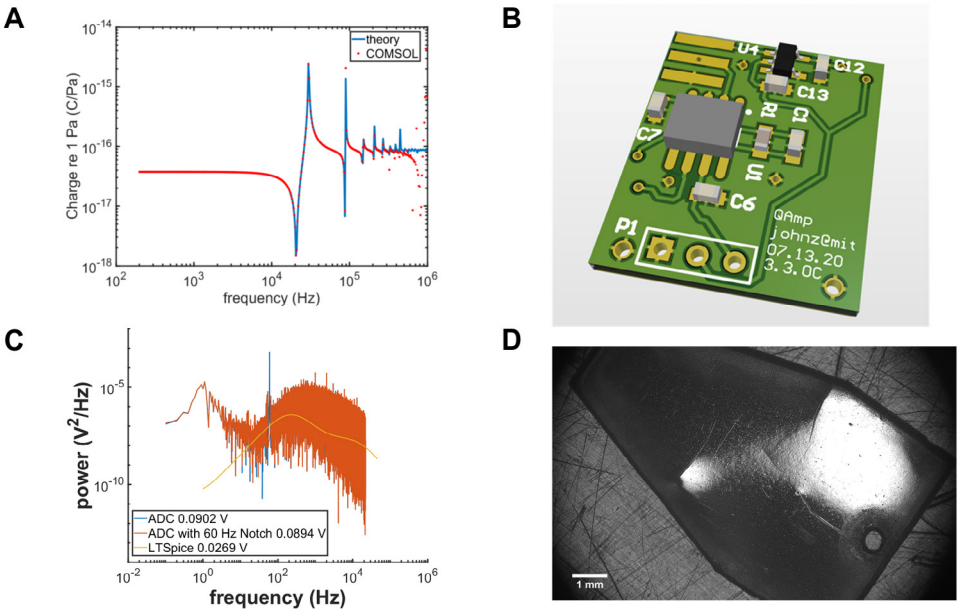

▲ Figure 1: Sensor modeling and amplifier design. (a) Frequency response of the device predicted by theory and our finite element model, (b) four-layer charge amplifier PCB, (c) LTSpice and measured noise of the charge amplifier, and (d) laser cut PVDF-TrFE for sensing intracochlear pressure.

FURTHER READING

- S. Park et al., "PVDF-Based Piezoelectric Microphone for Sound Detection Inside the Cochlea: Toward Totally Implantable Cochlear Implants," *Trends Hear.*, vol. 22, pp. 1–11, 2018.
- J. S. Yang and X. Zhang, "Extensional Vibration of a Nonuniform Piezoceramic Rod and High Voltage Generation," *Int. J. Appl. Electromagn. Mech.*, vol. 16, no. 1–2, pp. 29–42, 2002.
- J. Sirohi and I. Chopra, "Fundamental Understanding of Piezoelectric Strain Sensors," *J. Intell. Mater. Syst. Struct.*, vol. 11, no. 4, pp. 246–257, 2000.

Fluorescent Janus Droplet and Its Application in Biosensing of Listeria Monocytogenes

J. Li, S. Savagatrup, Z. Nelson, K. Yoshinaga, T. M. Swager
Sponsorship: NSF, DOD

Dynamic complex droplets afford versatile platforms for biosensing. The biosensing methods based on droplets enable a combination of advantages including speed, cost-effectiveness, and portability. This research explores a sensing method based on the agglutination of Janus emulsions for *Listeria monocytogenes*, which is a gram-positive bacterium and is responsible for a potentially lethal foodborne bacterial illness. We create a bio-recognition interface between the Janus emulsions that comprises equal volumes of hydrocarbon and fluorocarbon oils in Janus morphology by attaching antibodies to a functional surfactant polymer with a tetrazine/trans-cyclooctene (TCO) click reaction. The Listeria antibodies would be on the surface of the hydrocarbon hemisphere since the surfactant will stay at the interface of the hydrocarbon and water phase. Agglutinations of Janus droplets are formed when Listeria is added because of the strong binding between Listeria and the Listeria antibody located at the hydrocarbon surface of the emulsions. By incorporating one emissive dye in the fluorocarbon phase and a blocking dye in the hydrocarbon phase of Janus droplets, we conduct a two-dye assay, which enables the rapid detection of trace Listeria in two hours via an emissive signal produced in response to Listeria binding. To clarify, the Janus structures are tilted from their equilibrium position as a result of the formation of agglutinations and produce emissions that would ordinarily be obscured by a blocking dye. Overall, this method not only provides rapid and inexpensive Listeria detection with high sensitivity but also can be used to create a new class of biosensors by connecting with other related recognition elements.

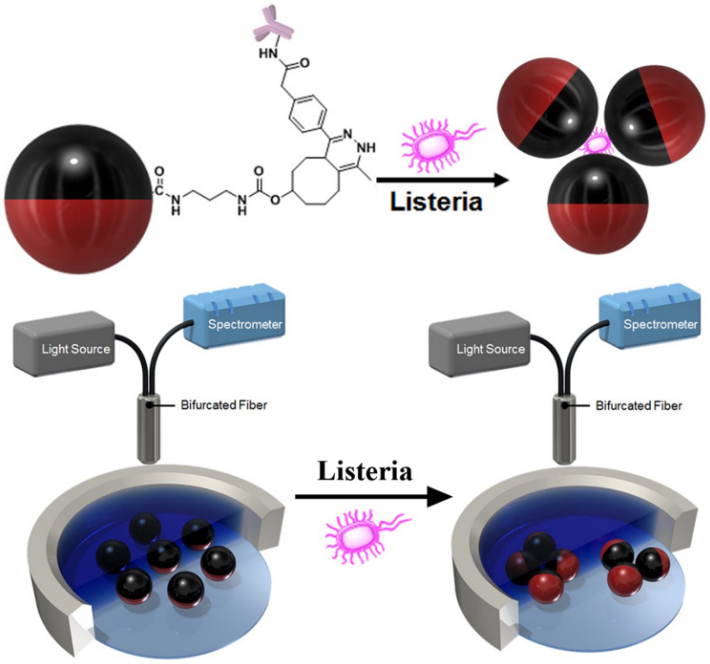

▲ Figure 1: Schematic of the agglutination assay of Janus emulsions for the biosensing of *Listeria Monocytogenes*.

Dance-Inspired Investigation of Human Movement

P. Namburi, L. Daniel, M. Feigin, Almon, B. Anthony, B. Moss, A. Kappacher
Sponsorship: NCSOFT

This research focuses on efforts to formalize a dancer's approach to movement. The overarching hypothesis is that dancers stabilize their joints through stretches – which are observed during common activities such as walking and running. However, most untrained individuals are able to apply this form of stabilization only during activities such as walking that seemingly "just happen," much as we "see." In contrast, the best dancers and athletes are able to generalize this stretch-based joint stabilization beyond walking to their art form. To understand how dancers organize movement through stretches, the researchers use motion tracking and electromyography. This work will potentially benefit several fields, including soft robotics, neuroscience, and AI.

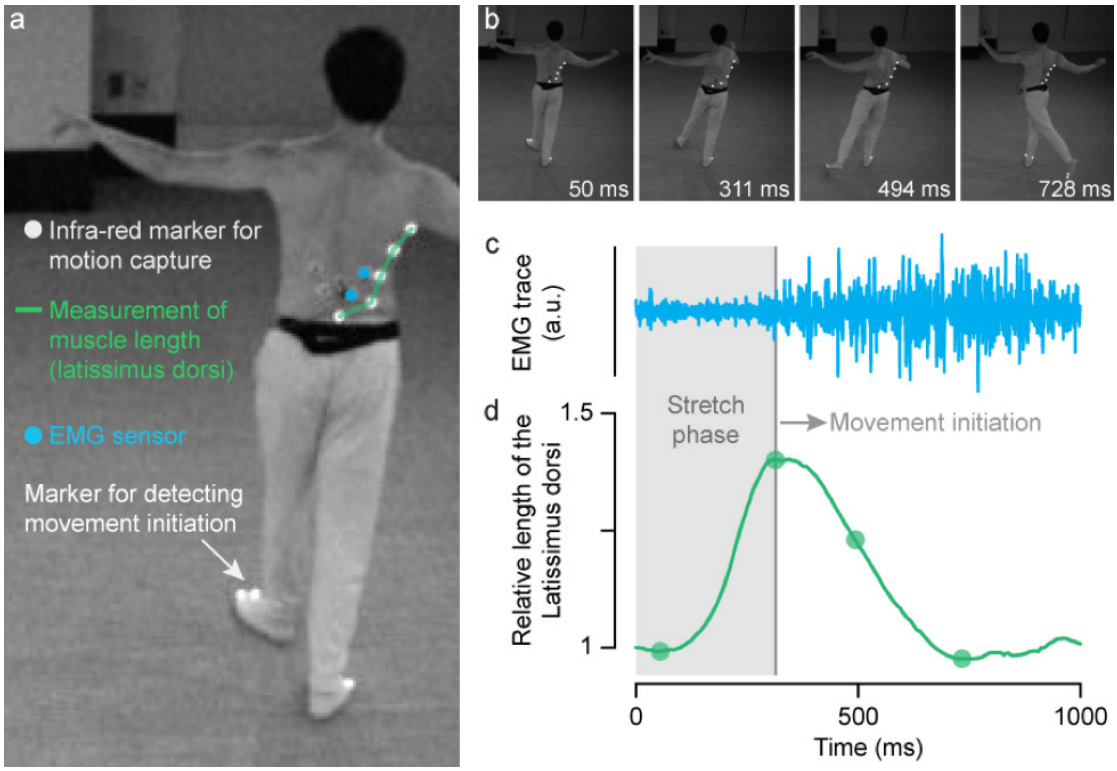

▲ Figure 1: ***a-b. Experiment.*** A dancer's movements were studied during the execution of a 'back ronde', i.e. a dance move that involves moving the left leg counter-clockwise while maintaining balance on the rightleg. Length and activity of the latissimus dorsi muscle were studied. To monitor stretches in the latissimus dorsi muscle, we used 3d motion capture technology at the MIT.nano Immersion Lab. Reflective infra-red markers (bright spots) were placed along the latissimus dorsi muscle to monitor its length (green line), and on the toes to measure initiation of movement. To measure the activation of the latissimus muscle, we used electromyography, and the position of the sensors is shown by blue circles. The four green circles in d correspond to the time points highlighted in the evolution of movement during the ronde, depicted in b.

c-d. Physiological measurements show two distinct phases of movement. An increase in EMG activity is detected starting ~300ms (c). This corresponds to when the movement is initiated (gray vertical line) as monitored by the movement of the big toe. Prior to activation of the latissimus dorsi muscle, we see an increase in its length (d). This 'stretch phase' is marked by the gray rectangle. Within the next 400ms, the leg reaches its destination during the 'execution phase.

Nanoscale Insights into the Mechanisms of Cellular Growth and Proliferation

K. B. Rogala, X. Gu, J. F. Kedir, M. Abu-Remaileh, L. F. Bianchi, A. M. S. Bottino, R. Dueholm, A. Niehaus, D. Overwijn, A-C. Priso Fils, S. X. Zhou, D. Leary, N. N. Laqtom, E. J. Brignole, D. M. Sabatini
Sponsorship: NIH, DoD, Lustgarten Foundation, Tuberous Sclerosis Association, MIT Koch Institute, Charles A. King Trust, Ibn Khaldun Fellowship, Howard Hughes Medical Institute, American Cancer Society

The growth and proliferation of human cells are controlled by the large molecular machine called mTORC1 that acts as a molecular equivalent of an AND logic gate. mTORC1 integrates multiple environmental signals, such as nutrients and growth factors, and orders the cell to either grow and divide in times of plenty or stand by and recycle when nutrients are scarce. Using electron cryomicroscopy, we revealed how mTORC1 recognizes nutrient signals, which provided a nanoscale-precision blueprint for the design of therapies aimed at deregulated mTORC1 in diseases of cellular growth, such as cancer.

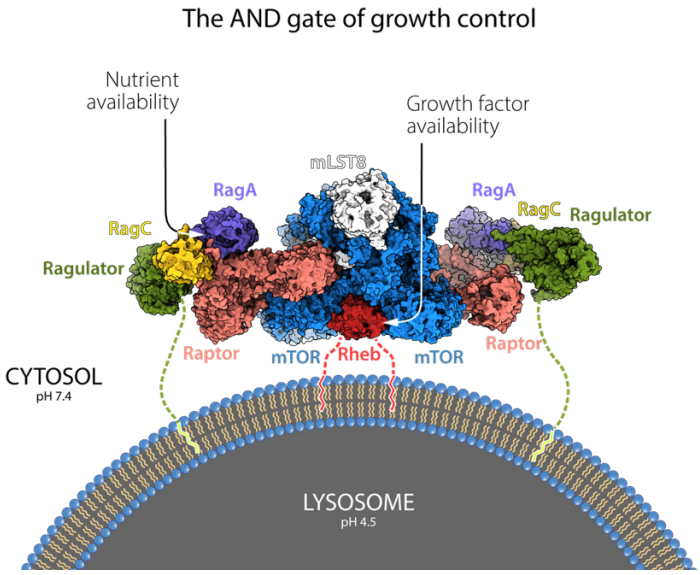

▲ Figure 1: Figure: The mTORC1 kinase fully docked on the lysosomal surface via its association with two classes of GTPase proteins: Rags and Rheb. Together, these two GTPases constitute an AND gate for mTORC1 signaling, relaying the presence or absence of two input signals: (1) nutrients and (2) growth factors.

FURTHER READING

- K.B. Rogala, D. M. Sabatini, et al., "Structural Basis for the Docking of mTORC1 on the Lysosomal Surface", *Science*, 25 Oct 2019 : 468-475 https://science.sciencemag.org/content/366/6464/468.abstract
- K. Shen, K. B.Rogala, D. M. Sabatini et al., "Cryo-EM Structure of the Human FLCN-FNIP2-Rag-Ragulator Complex", *Cell*, Volume 179, Issue 6, 2019, https://doi.org/10.1016/j.cell.2019.10.036